Hindawi
Journal of Nanomaterials
Volume 2019, Article ID 9827625, 9 pages
https://doi.org/10.1155/2019/9827625

Research Article

In Vitro Safety Evaluation and In Vivo Imaging Studies of Superparamagnetic Iron Oxide Nanoparticles through Biomimetic Modification

Xinfeng Song,[1] Yancong Zhang,[2,3] Hanwen Sun,[1] Pingxuan Dong,[1] Zhongyu Zhang,[1] and Jing Liu[1]

[1]*Shandong Provincial Engineering Laboratory of Novel Pharmaceutical Excipients, Sustained and Controlled Release Preparations, College of Medicine and Nursing, Dezhou University, Decheng District, Dezhou 253023, China*
[2]*Dezhou People's Hospital, Decheng District, Dezhou 253014, China*
[3]*School of Stomatology, Shandong University, China*

Correspondence should be addressed to Hanwen Sun; hanwen916@163.com

Received 26 July 2018; Revised 20 September 2018; Accepted 8 November 2018; Published 6 February 2019

Guest Editor: Manikandan Muthu

Copyright © 2019 Xinfeng Song et al. This is an open access article distributed under the Creative Commons Attribution License, which permits unrestricted use, distribution, and reproduction in any medium, provided the original work is properly cited.

Magnetic resonance imaging (MRI) is an advanced medical imaging diagnostic technique that utilizes different resonance signals generated by the signal strength of water content and the relaxation time of protons in water molecules under the influence of an external magnetic field. This technique requires contrast agents, such as Gd-DTPA and Gd-DOTA, which could increase the risk of renal fibrosis in patients with severe renal insufficiency. The magnetic moment or susceptibility of superparamagnetic iron oxide nanoparticle (SPION) is higher than that of other paramagnetic substances and could significantly reduce the dosage of the contrast agent required. In our previous work, the novel magnetic composite nanoparticles (abbreviated as c(RGDyK)-PDA-SPION) had been successfully synthesized by a facile and simple approach. Further evaluation had demonstrated that it had an average particle size of about 50 nm and uniform distribution, superparamagnetic properties, and good dispersion stability in water solution. Animal acute toxicity test also had proved that it had high safety in vivo. In this work, c(RGDyK)-PDA-SPION was further studied for the cell toxicity and effect on HepG2 cells in vitro, and the MRI imaging of this contrast agent in HepG2 tumor-bearing mice was also studied. It is an extension of the published work. The results showed that it possessed high safety and enrichment phenomenon on HepG2 cells in vitro. Animal experimental data preliminarily prove that the contrast agent could enhance the MRI T_2-weighted imaging capability of HepG2 carcinoma in tumor-bearing mice and could be a potential T_2 contrast agent.

1. Introduction

Magnetic resonance imaging (MRI), which was first proposed by Lauterbur in 1973 [1], is an advanced medical imaging diagnostic technique that utilizes different resonance signals generated by the signal strength of water content and the relaxation time of protons in the water molecules under the influence of an external magnetic field [2]. In clinical practice, the relaxation time of different healthy or tumor tissues overlaps with one another, leading to difficult diagnosis. Thus, researchers investigated the use of contrast agents to enhance the signal contrast and improve the resolution of soft tissue images. At present, more than 30% of MRI examinations require the use of an MRI contrast agent [3]. By shortening the proton relaxation times T_1 and T_2, an MRI contrast agent can improve the signal differences of different organizations or pathological changes and thus facilitate the diagnosis of lesions.

The paramagnetic metal ion Gd^{3+} contains seven unpaired electrons; as such, the ion possesses large electron spin magnetic moment, relaxation efficiency, and symmetric electric field and can easily coordinate with seven to eight water molecules. Gd^{3+} has become the best choice for T_1 MRI contrast agent [4, 5]. However, Gd^{3+} easily accumulates

in the human liver, spleen, bone, and brain and is highly toxic because of its ionic form [6, 7]. Therefore, scholars must explore suitable ligands that can form complexes with Gd^{3+} to reduce its toxicity.

In 1983, Yim et al. [8] applied Gd-DTPA to diagnose brain tumors for the first time; this contrast agent has been widely used after securing FDA certification in 1987. However, Gd-DTPA can produce high osmotic pressure in the form of sodium or glucosamine ions. In this regard, many nonionic Gd-DTPA derivatives have been synthesized. To date, Gd-DOTA is the most stable gadolinium coordination contrast agent [9]. However, at the end of 2006, the FDA issued a warning stating that gadolinium contrast agents could increase the risk of renal fibrosis in patients with severe renal insufficiency [10, 11].

As a T_2 MRI contrast agent, superparamagnetic contrast agents are usually composed of a nanometer-sized iron oxide crystal nucleus and a stable coating material. The core of the iron oxide crystal is typically Fe_3O_4, γ-Fe_2O_3, or FeOOH [12]. Among these substances, SPION has attracted increasing attention because of its higher magnetic moment and susceptibility ratio than other paramagnetic materials; moreover, the relaxation efficiency of the hydrogen nucleus after entering the tissue could significantly reduce the dosage of the contrast agent required [13]. However, naked SPION easily coagulates, exhibits large particle sizes, and is poorly dispersed because of its surface hydrophobicity, high surface energy, and magnetic field influence, which prevent the particles to pass through capillaries and into tissues; as such, naked SPION has limited biomedical applications [14]. These issues are circumvented by using physical or chemical methods to modify the particle surface. The most common coating materials are dextran, glucan derivatives, starch, silicone oil, arabic galactose, and albumin.

A literature review on SPION surface modification revealed that most preparation methods are relatively complicated and require strict procedures. Therefore, the preparation and surface functionalization of SPION is a key step for solving the limited application of magnetic nanomaterials. Dopamine (DA) is the main component of the adhesion protein of mussel, and its homopolymer is extremely adhesive and can modify the surface coating of various materials [15, 16]. Researchers have used the self-polymerization and super adhesion properties of DA to create various hydrophilic composite materials [17, 18]. However, few studies have investigated the surface modification of SPION by using DA and MRI imaging. In a previous work [19] (J Nanosci Nanotechnol. 2016. http://www.aspbs.com/jnn/), c(RGDyK)-PDA-SPION was successfully synthesized. Preliminary results demonstrated that the particles of c(RGDyK)-PDA-SPION are about 50 nm in size and are distributed evenly; the particles possess significant magnetic properties, good water dispersibility, and high internal security. Given its superior performance, c(RGDyK)-PDA-SPION was further studied for its in vitro cell toxicity and in vitro enrichment effect on HepG2. The in vivo MRI imaging law of this contrast agent in HepG2 tumor-bearing mice was discussed in this paper.

2. Methods and Materials

2.1. Reagents and Instruments. SPION, PDA-SPION, c(RGDyK)-PDA-SPION (prepared by our laboratory), trypsin, EDTA, DMSO, MTT, RPMI 1640 medium, fetal bovine serum (Shanghai Yuanye Bio-Technology Co. Ltd.), hepatocellular carcinoma cell line HepG2 (Institute of Basic Medicine, Chinese Academy of Medical Sciences), Prussian blue stain kit (Beijing Solarbio Science & Technology Co. Ltd.), and HepG2 tumor-bearing mice (Shanghai Ruantuo Biotechnology Co. Ltd.) were used in this study.

A CO_2 incubator (Thermo HERAcell 240i), a full-wavelength multifunctional enzyme marker (Thermo Varioskan Flash), an inverted fluorescence microscope (Leica, DMI3000B), and a small nuclear magnetic resonance apparatus (Suzhou Niumag Analytical Instrument Corporation, MesoMR23-060H-I) were also adopted.

2.2. Cytotoxicity of Magnetic Nanoparticles. HepG2 cells were cultured and used to investigate the cytotoxicity of three kinds of particles to human liver cells. The effects of the three types of nanoparticles on the activity of HepG2 cells were studied by MTT experiment. The inoculation density of HepG2 cells in the logarithmic growth phase was 4.7×10^5/mL. After the cells became adherent, the supernatants of the intervention groups were mixed with different concentrations of serum-free mixture containing different surface-modified magnetic nanoparticles (SPION, PDA-SPION, and c(RGDyK)-PDA-SPION). Three particle concentration gradients, namely, 5, 10, and 20 μg/mL, were applied. A blank control group was used and added only with serum-containing RPMI 1640 medium. The cell suspensions were then cultured at 37°C and 5% CO_2 in an incubator for 24 h. Each hole was added with 15 μL of MTT and 85 μL of PBS. After 4 h, the culture plate was removed from the incubator, and the supernatant was discarded. Each hole was added with DMSO (100 μL), and 490 nm wavelength was used to determine the absorbance value (optical density (OD)) of each aperture.

2.3. In Vitro Cell Targeting Enrichment Effect of Magnetic Nanoparticles. We then determined the concentrations of the SPION, PDA-SPION, and c(RGDyK)-PDA-SPION magnetic nanoparticles in hepatoma cells. The concentrations of the RPMI 1640 culture medium without serum were 2, 5, and 10 μg/mL for the three magnetic nanoparticle-exposed liquids of SPION, PDA-SPION, and c(RGDyK)-PDA-SPION. HepG2 cells in the logarithmic growth stage were inoculated at a cell density of 4.7×10^5/mL and in a six-hole cell culture plate with a cover glass. The cells were cultured at 37°C in a 5% CO_2 incubator. After the cells were adherent for 24 h, different concentrations of the three magnetic nanoparticle-exposed liquids and a blank control group composed of only serum-containing RPMI 1640 medium were added separately and incubated for 24 h. The magnetic nanoparticles were then observed in the liver cancer cells.

Based on the enrichment effect, 10 μg/mL was selected for SPION-, PDA-SPION-, and c(RGDyK)-PDA-SPION-exposed liquids. In the logarithmic phase, 4.7×10^5/mL HepG2

cells were inoculated in a six-hole cell culture plate with a cover and incubated at 37°C in a 5% CO_2 incubator. After the cells adhered to the wall and the exposed liquids were added, exposure was performed for 6, 12, 24, and 48 h. The cells were fixed with 4% paraformaldehyde for 20 min, dried, cleaned with PBS, and subjected to 10% Prussian blue staining ($K_4Fe(CN)_6 \cdot 3H_2O$) and nuclear solid red staining. The samples were sealed with neutral resin, observed under an inverted microscope and photographed.

2.4. T_2 Relaxation Time Test of Magnetic Nanoparticles. The resonant frequency of the small nuclear magnetic resonance instrument (MesoMR23-060H-I) was 23 MHz, the magnetic strength was 0.5 T, the coil diameter was 60 mm, and the magnetic temperature was 32.0°C. The three magnetic nanoparticles of SPION, PDA-SPION, and c(RGDyK)-PDA-SPION were, respectively, assigned to concentrations of 10.449, 20.898, 41.797, 83.594, and 167.188 μg/mL. Five concentration gradient solutions were placed in the small nuclear magnetic resonance instrument coil for testing and analyzing T_2 relaxation time of the contrast agent with nuclear magnetic resonance analysis software.

2.5. In Vitro T_2-Weighted Imaging Test of Magnetic Nanoparticles. Debugging small nuclear magnetic resonance instrument (MesoMR23-060H-I) used resonant frequency of 23 MHz, magnet strength of 0.5 T, coil diameter of 60 mm, and magnet temperature of 32.0°C. Six concentration gradients (0, 10.449, 20.898, 41.797, 83.594, and 167.188 μg/mL) of the solutions of the three magnetic nanoparticles (SPION, PDA-SPION, and c(RGDyK)-PDA-SPION) were placed in the coil for detection. Imaging software and MSE sequence were used to collect images.

2.6. In Vivo MRI Imaging Test of Magnetic Nanoparticles in Normal Mice. In this experiment, the resonant frequency of the small nuclear magnetic resonance instrument (MesoMR23-060H-I) was 23 MHz, the magnetic strength was 0.5 T, the coil diameter was 60 mm, and the magnetic temperature was 32.0°C. The abdominal cavity of Kunming mice weighing 18–25 g was injected with 0.08 mL/10 g weight of 8% chloral hydrate. After anesthesia, 0.2 mL of 167.188 μg/mL each of the SPION, PDA-SPION, and c(RGDyK)-PDA-SPION magnetic nanoparticle solutions was injected through the tail vein. MRI signals were collected at 0, 0.5, 1, 2, and 24 h, and the coronal plane images of mice were recorded using MRI software and MSE sequence.

2.7. MRI Imaging Test of c(RGDyK)-PDA-SPION Contrast Agent in Tumor-Bearing Mice. A suspension of 1×10^7/mL HepG2 cells in the logarithmic phase was prepared in serum-free medium. Subsequently, 0.2 mL of the cell suspension was inoculated subcutaneously in the side hip of BALb/c nude mice. After 15 days, the tumors were about 0.8–1 cm in size.

The resonant frequency of the debug small nuclear magnetic resonance (MesoMR23-060H-I) was 23 MHz, the magnetic strength was 0.5 T, the coil diameter was 60 mm, and the magnetic temperature was 32.0°C. The abdominal cavity of tumor-bearing mice weighing 20 g was injected with 0.08 mL/10 g weight of 8% chloral hydrate. After anesthesia, 0.2 mL of 167.188 μg/mL of the c(RGDyK)-PDA-SPION nanoparticle solution was injected through the tail vein. The T_2-weighted enrichment of MRI imaging of the c(RGDyK)-PDA-SPION magnetic nanoparticle contrast agent was tested after 0, 0.5, 1, 2, 6, and 24 h in the cancer, liver, spleen, heart, and kidney tissues through nuclear magnetic resonance imaging software. The imaging effect of the tumor and the tissues and organs of the tumor-bearing mice was determined by unifying mapping and pseudo-color image processing. The optimum imaging times of the induced tumor and the tissues and organs were determined.

3. Results and Discussion

3.1. Cytotoxicity of the Magnetic Nanoparticles. The MTT experimental results showed that the three types of magnetic nanoparticles within the concentration range of 0–20 μg/mL showed no significant influence on the activity of HepG2 cells (Figure 1). Hence, the three kinds of nanoparticles were biocompatible and safe for liver cells within a controlled concentration range.

3.2. Enrichment Effect of Magnetic Nanoparticles In Vitro in HepG2 Cells. Studies shown that integrin $\alpha_v\beta_3$ is highly expressed on the surface of various malignant tumor cells [20], which plays a significant role in tumor growth, local infiltration, and metastasis, especially in tumor-induced angiogenesis. The c(RGDyK), an arginine-glycine-aspartic tripeptide sequence, could target specifically to intergrin $a_v\beta3$-rich tumor cells such as primary hepatocellular carcinoma [21, 22]. As shown in Figure 2, HepG2 cells were exposed to different concentrations of SPION solution. The amount of SPION in the hepatoma cells did not increase with increasing SPION concentration. Similarly, the content of PDA-SPION magnetic nanoparticles in HepG2 cells did not increase with increasing concentration of PDA-SPION magnetic nanoparticles. In contrast to SPION and PDA-SPION, the content of c(RGDyK)-PDA-SPION magnetic nanoparticles in HepG2 cells augmented upon exposure to different concentrations of c(RGDyK)-PDA-SPION magnetic nanoparticle-containing liquid for 24 h (Figure 2).

As shown in Figure 3, HepG2 cells were exposed to 10 μg/mL SPION magnetic particle solution. As the exposure time was prolonged, the content of SPION magnetic nanoparticle did not change significantly in HepG2 cells. Similarly, the content of PDA-SPION magnetic nanoparticles in HepG2 cells exposed to 10 μg/mL PDA-SPION magnetic nanoparticle solution showed no significant changes. The content of c(RGDyK)-PDA-SPION magnetic particles in HepG2 cells did not significantly increase with prolonged exposure to c(RGDyK)-PDA-SPION magnetic particle-containing liquid. Given the surface bonding of SPION magnetic nanoparticles to the specific molecular target c(RGDyK), the targeting effect of c(RGDyK)-PDA-SPION magnetic nanoparticles on liver cancer cells enhanced the enrichment effect of the agent on the cells. This effect may be enhanced by increasing the concentration and extending the exposure time.

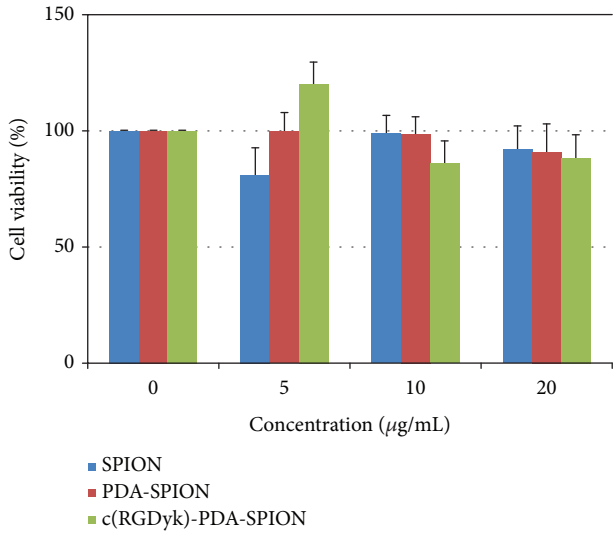

Figure 1: The MTT assay on the effects of three magnetic nanoparticles on HepG2 cells. HepG2 cells were exposed to 0, 5, 10, and 20 μg/mL SPION, PDA-SPION, and c(RGDyK)-PDA-SPION magnetic nanoparticles for 24 hours. Three magnetic nanoparticles all showed no significant effects on HepG2 cells.

3.3. T_2 Relaxation Time of Magnetic Nanoparticles. The process of nuclei returning from an excited state to an equilibrium state is called relaxation. The time which it takes is called relaxation time. There are two types of relaxation time, namely, T_1 and T_2. T_1 is spin-lattice or longitudinal relaxation time, and T_2 is spin-spin or transverse relaxation time, which depends on the proton density in the tissues [23]. The magnetic moment and the magnetic susceptibility of SPION are greater than the human body structure. When water molecules diffusing through them and interacting with the proton, the proton transverse magnetization phase changes and accelerates the process of phase, which makes T_2 of the proton shortened [24]. As shown in Table 1, increasing concentrations of the three magnetic nanoparticle contrast agents resulted in decreased T_2 relaxation time. The variation trend in the c(RGDyK)-PDA-SPION contrast group was more pronounced than those of the SPION and PDA-SPION contrast groups. Hence, c(RGDyK)-PDA-SPION exhibited better imaging capability than the two other magnetic nanoparticles and can be used as a good MRI T_2 contrast agent.

3.4. In Vitro T_2-Weighted Imaging of Magnetic Nanoparticles. A T_2-weighted image highlights the relaxation time T_2 and can be divided into grayscale and pseudo-color images. The grayscale is darker, and the relaxation time T_2 is shorter. The pseudo-color images are bluer, and the relaxation time T_2 is shorter. As shown in Figure 4, the grayscale color progressively darkened, and the color in the pseudo-color image slanted blue with increasing concentration of the three kinds of magnetic nanoparticles. Hence, the shortened T_2 relaxation time corresponded with increasing concentration of the three kinds of magnetic nanoparticles. The imaging pattern of the c(RGDyK)-PDA-SPION contrast agent group was more prominent than those of the SPION and PDA-SPION contrast agent groups. After SPION coupled with c(RGDyK), aggregation was prevented to a certain extent. The color gradient of the c(RGDyK)-PDA-SPION contrast group consequently became evident, which revealed that it was more suitable than the other particles as T_2 contrast agent.

3.5. In Vivo MRI Imaging of Magnetic Nanoparticles in Normal Mice. In the coronal plane T_2-weighted images (Figure 5), the liver tissue of the normal mice given with the SPION contrast agent began to darken in 30 min (pseudo-color became blue), and the color change was the most obvious after 1 h. The color of the liver tissue faded (pseudo-color blue faded) at 2 h. In the PDA-SPION contrast agent group, changes were observed in the coronal plane T_2-weighted images of liver tissues compared with those in normal mice 24 h after PDA-SPION was injected via the tail vein. From the gray image, a slight dimming appeared in the liver tissue at 30 min (pseudo-color became blue). The imaging effect was the most obvious at 60 min, and the color of the liver began to fade (pseudo-color blue faded) at 120 min. Finally, the color of the liver tissue was basically restored after 24 h to that before the contrast agent was injected. For the c(RGDyK)-PDA-SPION contrast agent group, changes were noted in the coronal plane T_2-weighted image of the liver tissues of the normal mice after c(RGDyK)-PDA-SPION was injected through the tail vein. In the gray image, the liver tissue began to darken (pseudo-color became blue) at 30 min, and the color change was the most obvious at 60 min. After 24 h, the color of the liver tissue was basically restored to that before the c(RGDyK)-PDA-SPION contrast agent was injected.

Experimental results showed that the enrichment effects of the three contrast agents on the liver were stronger than that on any other organ. Within 1 h, the maximum concentration of the three types of particles was achieved in the liver; the most obvious color change was also observed in the liver relative to the surrounding tissue. The color change abated and basically recovered after 24 h to the color before the injection. Thus, in the c(RGDyK)-PDA-SPION contrast agent group, the best liver imaging acquisition time was about 1 h. The basic metabolism of the particle in the liver was completed within 24 h. The results provide experimental basis for in vivo study of the c(RGDyK)-PDA-SPION contrast agent in tumor-bearing mice.

3.6. MRI Imaging of c(RGDyK)-PDA-SPION Contrast Agent in Tumor-Bearing Mice. As shown in the grayscale and pseudo-color images of Figure 6, after the tail vein injection of c(RGDyK)-PDA-SPION contrast agent, T_2-weighted imaging of a tumor-burdened mouse liver and tumor showed variation law with prolonged time after injection of the contrast agent into the tumor-burdened mouse liver. The tumor tissues were gray in the grayscale image and bright blue in the pseudo-color image. The gray color of the liver tissue in the grayscale image and the blue color in the pseudo-color images became deepest at 60 min. After 2 h, the gray color of the grayscale image lightened, and the blue color of the

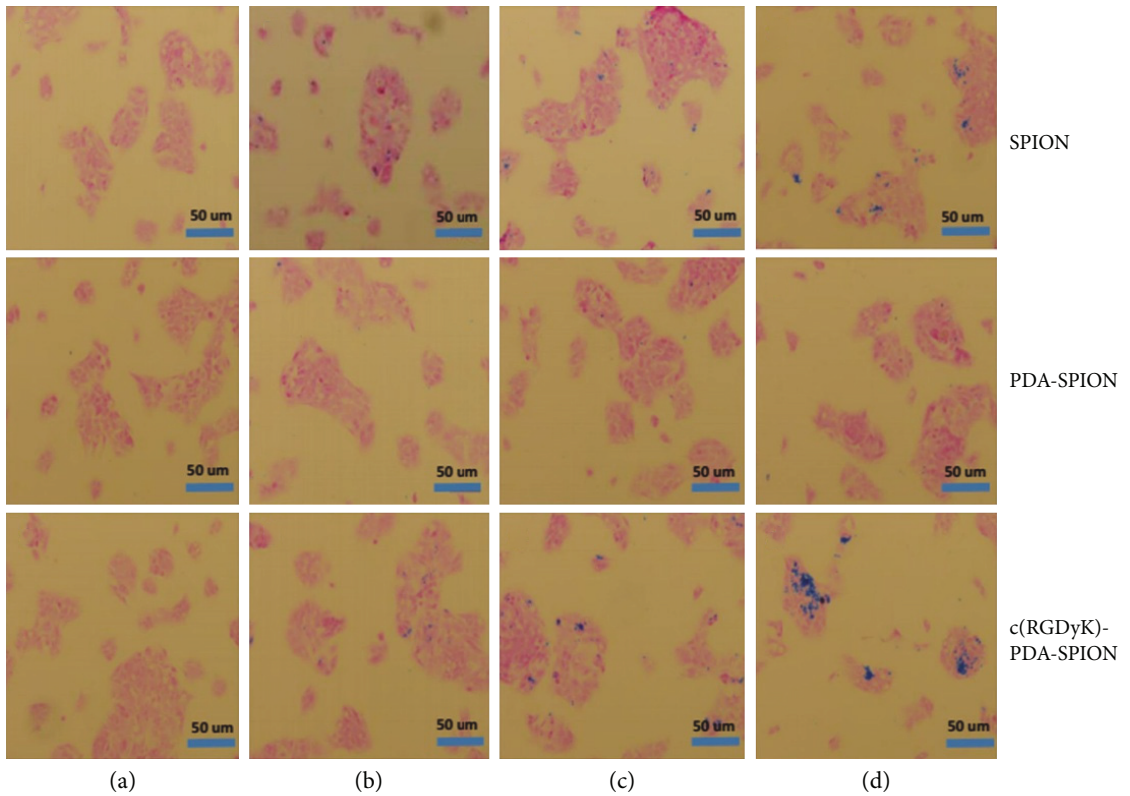

Figure 2: HepG2 cells were exposed to 0 (a), 2 (b), 5 (c), and 10 μg/mL (d) SPION, PDA-SPION, and c (RGDyK)-PDA-SPION magnetic nanoparticles for 24 hours. Enrichment results of magnetic nanoparticles in HepG2 cells were detected.

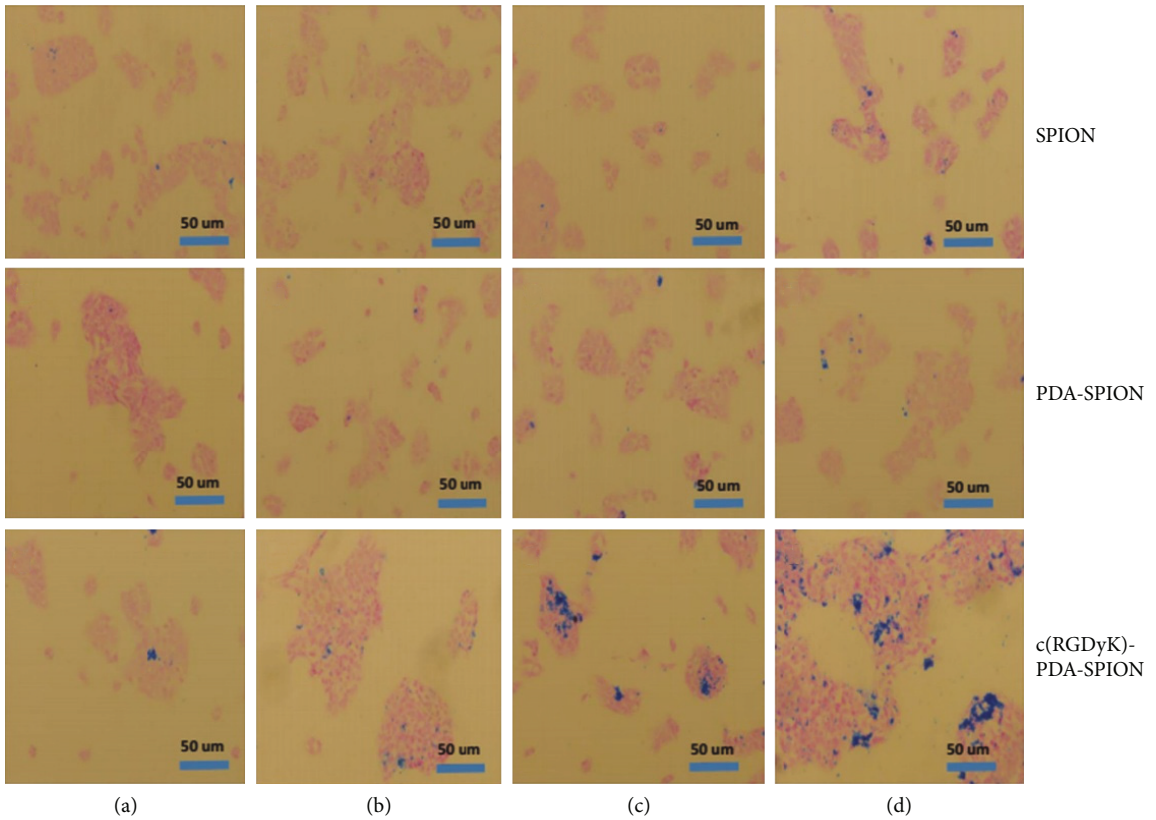

Figure 3: HepG2 cells were exposed to 10 μg/mL SPION, PDA-SPION, and c (RGDyK)-PDA-SPION magnetic nanoparticles for 6 (a), 12 (b), 24 (c), and 48 hours (d). Enrichment results of magnetic nanoparticles in HepG2 cells were detected.

Table 1: T_2 relaxation time shorten of SPION, PDA-SPION, and c(RGDyK)-PDA-SPION, with the concentrations increasing.

T_2 (ms)	Concentration (μg/mL)				
	10.449	20.898	41.797	83.594	167.188
SPION group	159.873	116.743	81.228	50.084	29.506
PDA-SPION group	241.383	208.930	120.440	72.596	37.770
c(RGDyK)-PDA-SPION group	94.364	63.525	42.030	22.070	11.692

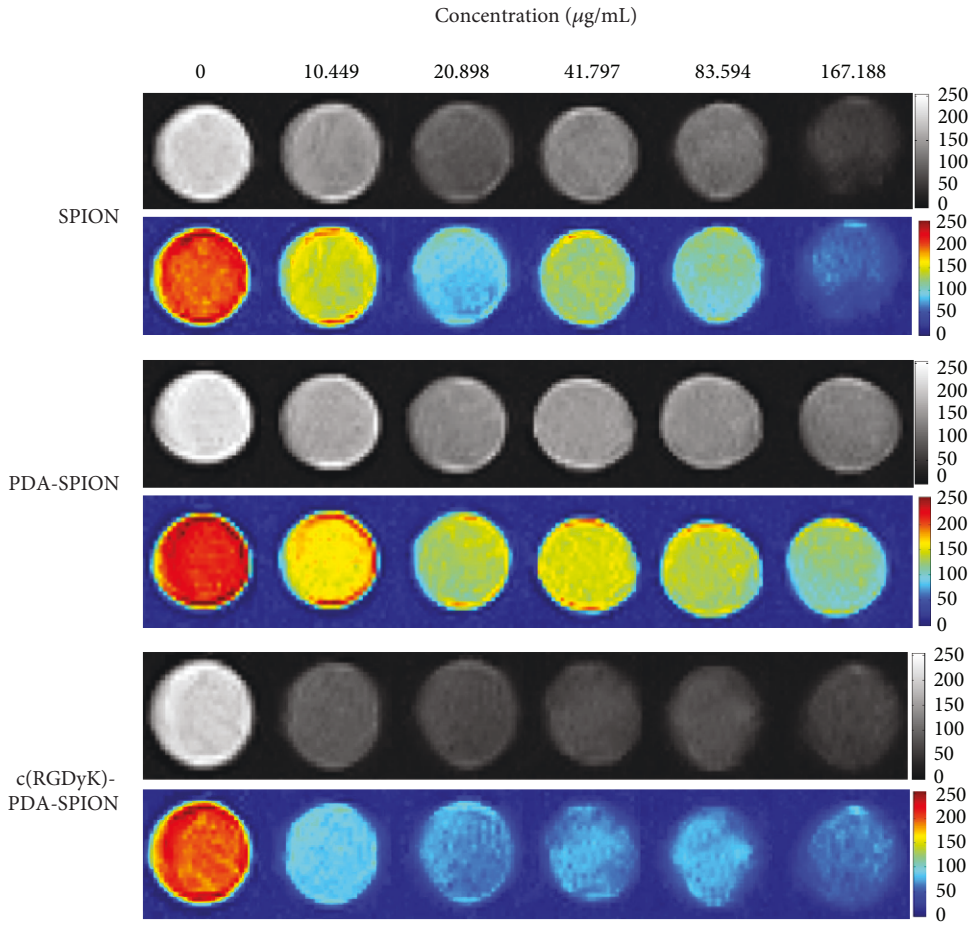

Figure 4: In vitro T_2-weighted image of three magnetic nanoparticles, namely, SPION, PDA-SPION, and c(RGDyK)-PDA-SPION. In the T_2-weighted MR image, the c(RGDyK)-PDA-SPION displayed a significant signal reduction with increasing nanoparticle concentration.

pseudo-color images became pale blue; these changes revealed that the c(RGDyK)-PDA-SPION contrast agent in the liver has an optimal imaging time of 60 min. The results and preliminary experimental results were unified.

For tumor tissues in the tumor-bearing mice (Figure 6), the gray color of the grayscale image reached its deepest and the blue color of the pseudo-color images reached the darkest 2 h after tail vein injection. The gray color of the grayscale image lightened, and the blue color of the pseudo-color image became red after 6 h. These results suggest that 2 h may be the best imaging time, which is about 1 h later than that of the liver. Given the growth of tumor inside the skin rather than in in situ liver cancer, the penetration of the c(RGDyK)-PDA-SPION contrast agents into the tumor tissue was difficult through the tumor blood vessels. This difference delayed the optimal imaging time. The above experimental results need to be further studied in an in situ liver cancer model.

4. Conclusion

In summary, a nanoparticle named c(RGDyK)-PDA-SPION with a particle size of about 50 nm had been successfully prepared in our previous work. In this work, c(RGDyK)-PDA-SPION was further investigated. We found that the c(RGDyK)-PDA-SPION displayed a significant signal reduction with increasing nanoparticle concentration, and they were nontoxic at lower concentrations from 5 to 20 μg/mL, and they had significant targeting effect of c(RGDyK)-PDA-SPION on liver cancer cells. The animal experiment

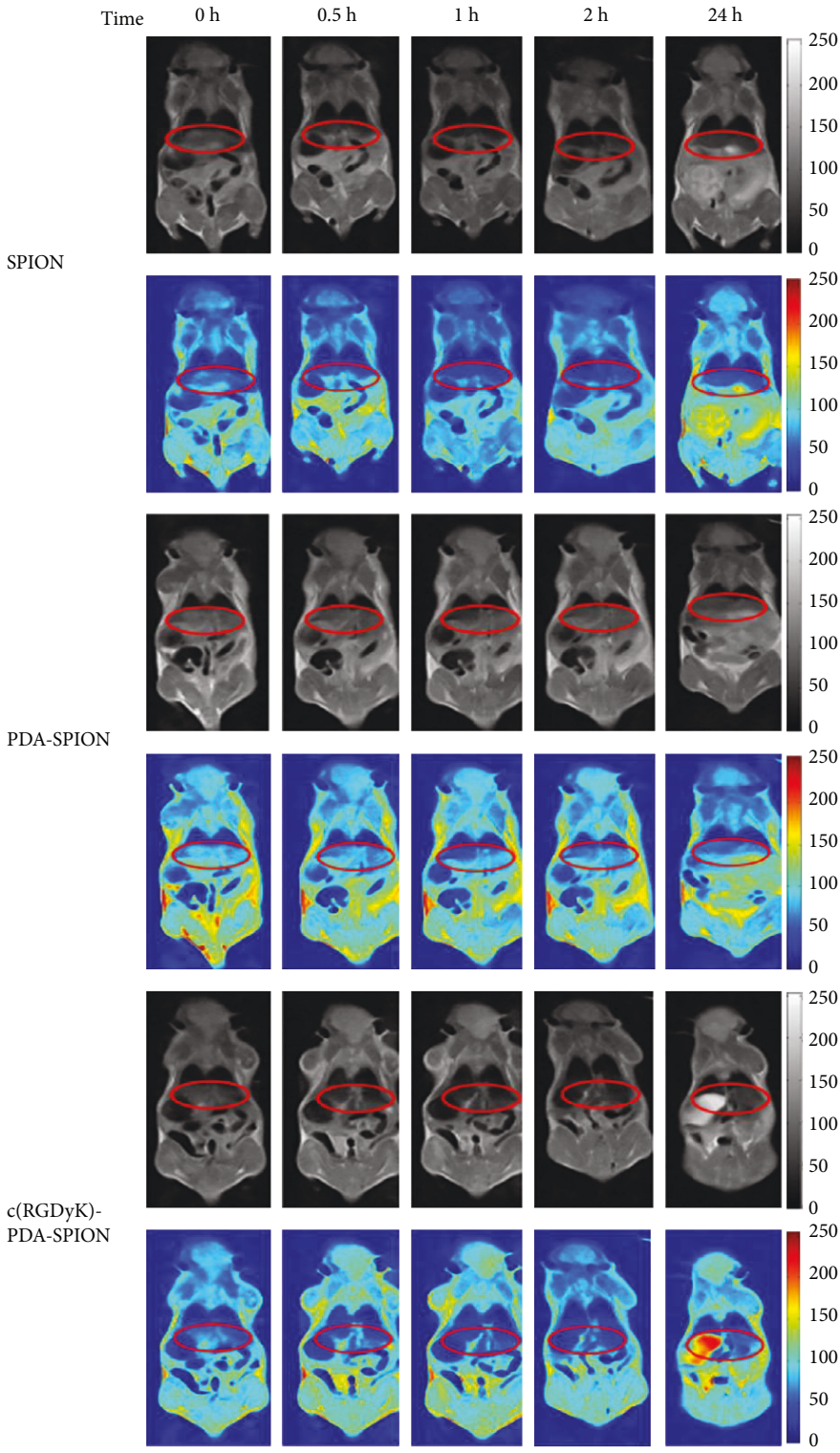

FIGURE 5: T_2-weighted image of three magnetic nanoparticles, namely, SPION, PDA-SPION, and c(RGDyK)-PDA-SPION. The T_2-weighted image change of SPION, PDA-SPION, and c(RGDyK)-PDA-SPION on the liver tissue of the normal mice (ellipse labeled as liver). The enrichment effects of the three magnetic nanoparticles on the liver were significant compared to the other organs. At about one hour, the maximum concentration of the three particles accumulated in the liver and was almost completely cleared about 24 hours.

results showed that the maximum concentration of the particles accumulated in the liver was at about one hour, and they were almost completely cleared about 24 hours. Further animal experiments have shown that they could enhance the MRI T_2-weighted imaging capability of tumor-burdened, and two hours was probably the best imaging time. Animal

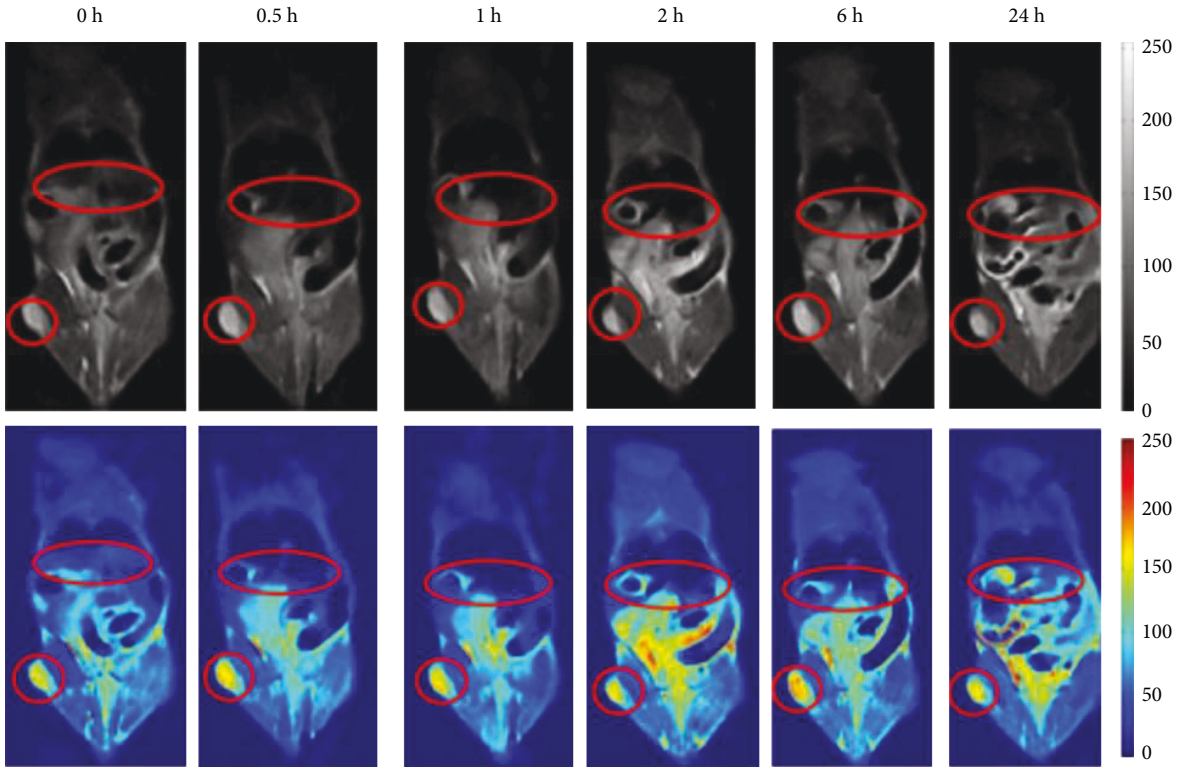

Figure 6: C(RGDyK)-PDA-SPION contrast agent tumor-bearing mice with T_2-weighted image. The T_2-weighted image changes of C(RGDyK)-PDA-SPION on the liver tissue and the tumor tissue of the tumor-bearing mice (ellipse labeled as liver, circle labeled as tumor). Two hours is probably the best imaging time of C(RGDyK)-PDA-SPION in the tumor, which was about one hour later than the optimal liver imaging time.

experimental data preliminarily proved that this contrast agent can enhance the MRI T_2-weighted imaging of HepG2 human hepatocellular carcinoma in mice and is a potentially good T_2 contrast agent.

Data Availability

The figure and table data used to support the findings of this study are included within the article.

Disclosure

Xinfeng Song and Yancong Zhang are the co-first authors.

Conflicts of Interest

The authors declare that there is no conflict of interests regarding the publication of this paper.

Acknowledgments

We are grateful to the National Natural Science Foundation of China (no. 51273033).

References

[1] P. C. Lauterbur, "Image formation by induced local interactions: examples employing nuclear magnetic resonance," *Nature*, vol. 242, no. 5394, pp. 190-191, 1973.

[2] D. Rugar, C. S. Yannoni, and J. A. Sidles, "Mechanical detection of magnetic resonance," *Nature*, vol. 360, no. 6404, pp. 563–566, 1992.

[3] P. Caravan, J. J. Ellison, T. J. McMurry, and R. B. Lauffer, "Gadolinium(III) chelates as MRI contrast agents: structure, dynamics, and applications," *Chemical Reviews*, vol. 99, no. 9, pp. 2293–2352, 1999.

[4] T. Kanda, K. Ishii, H. Kawaguchi, K. Kitajima, and D. Takenaka, "High signal intensity in the dentate nucleus and globus pallidus on unenhanced T1-weighted MR images: relationship with increasing cumulative dose of a gadolinium-based contrast material," *Radiology*, vol. 270, no. 3, pp. 834–841, 2014.

[5] D. A. Stojanov, A. Aracki-Trenkic, S. Vojinovic, D. Benedeto-Stojanov, and S. Ljubisavljevic, "Increasing signal intensity within the dentate nucleus and globus pallidus on unenhanced T1W magnetic resonance images in patients with relapsing-remitting multiple sclerosis: correlation with cumulative dose of a macrocyclic gadolinium-based contrast agent, gadobutrol," *European Radiology*, vol. 26, no. 3, pp. 807–815, 2016.

[6] T. Kanda, T. Fukusato, M. Matsuda et al., "Gadolinium-based contrast agent accumulates in the brain even in subjects without severe renal dysfunction: evaluation of autopsy brain specimens with inductively coupled plasma mass spectroscopy," *Radiology*, vol. 276, no. 1, pp. 228–232, 2015.

[7] H. Wei, O. T. Bruns, M. G. Kaul et al., "Exceedingly small iron oxide nanoparticles as positive MRI contrast agents," *Proceedings of the National Academy of Sciences of the United States of America*, vol. 114, no. 9, pp. 2325–2330, 2017.

[8] H. Yim, S. G. Yang, Y. S. Jeon et al., "The performance of gadolinium diethylene triamine pentaacetate-pullulan hepatocyte-specific T1 contrast agent for MRI," *Biomaterials*, vol. 32, no. 22, pp. 5187–5194, 2011.

[9] C. U. Herborn, E. Honold, M. Wolf et al., "Clinical safety and diagnostic value of the gadolinium chelate gadoterate meglumine (Gd-DOTA)," *Investigative Radiology*, vol. 42, no. 1, pp. 58–62, 2007.

[10] T. Grobner, "Gadolinium-a specific trigger for the development of nephrogenic fibrosing dermopathy and nephrogenic systemic fibrosis?," *Nephrology, Dialysis, Transplantation*, vol. 21, no. 4, pp. 1104–1108, 2006.

[11] W. A. High, R. A. Ayers, J. Chandler, G. Zito, and S. E. Cowper, "Gadolinium is detectable within the tissue of patients with nephrogenic systemic fibrosis," *Journal of the American Academy of Dermatology*, vol. 56, no. 1, pp. 21–26, 2007.

[12] Y. X. J. Wang, S. M. Hussain, and G. P. Krestin, "Superparamagnetic iron oxide contrast agents: physicochemical characteristics and applications in MR imaging," *European Radiology*, vol. 11, no. 11, pp. 2319–2331, 2001.

[13] R. Qiao, C. Yang, and M. Gao, "Superparamagnetic iron oxide nanoparticles: from preparations to in vivo MRI applications," *Journal of Materials Chemistry*, vol. 19, no. 35, pp. 6274–6293, 2009.

[14] A. Zhu, L. Yuan, and T. Liao, "Suspension of Fe_3O_4 nanoparticles stabilized by chitosan and o-carboxymethylchitosan," *International Journal of Pharmaceutics*, vol. 350, no. 1-2, pp. 361–368, 2008.

[15] H. G. Silverman and F. F. Roberto, "Understanding marine mussel adhesion," *Marine Biotechnology*, vol. 9, no. 6, pp. 661–681, 2007.

[16] H. Lee, S. M. Dellatore, W. M. Miller, and P. B. Messersmith, "Mussel-inspired surface chemistry for multifunctional coatings," *Science*, vol. 318, no. 5849, pp. 426–430, 2007.

[17] H. Lee, Y. Lee, A. R. Statz, J. Rho, T. G. Park, and P. B. Messersmith, "Substrate-independent layer-by-layer assembly by using mussel-adhesive-inspired polymers," *Advanced Materials*, vol. 20, no. 9, pp. 1619–1623, 2008.

[18] Y. Liao, Y. Wang, X. Feng, W. Wang, F. Xu, and L. Zhang, "Antibacterial surfaces through dopamine functionalization and silver nanoparticle immobilization," *Materials Chemistry and Physics*, vol. 121, no. 3, pp. 534–540, 2010.

[19] X. Song, X. Gu, H. Sun, C. Fu, Y. Zhang, and P. Dong, "Biomimetic modification and *in vivo* safety assessment of superparamagnetic iron oxide nanoparticles," *Journal of Nanoscience and Nanotechnology*, vol. 16, no. 4, pp. 4100–4107, 2016.

[20] H. Zhao, J. C. Wang, Q. S. Sun, C. L. Luo, and Q. Zhang, "RGD-based strategies for improving antitumor activity of paclitaxel loaded liposomes in nude mice xenografted with human ovarian cancer," *Journal of Drug Targeting*, vol. 17, no. 1, pp. 10–18, 2009.

[21] J. Xie, K. Chen, H.-Y. Lee et al., "Ultrasmall c(RGDyK)-coated Fe_3O_4 nanoparticles and their specific targeting to integrin $\alpha_v\beta_3$-rich tumor cells," *Journal of the American Chemical Society*, vol. 130, no. 24, pp. 7542-7543, 2008.

[22] J.-P. Xiong, T. Stehle, R. Zhang et al., "Crystal structure of the extracellular segment of integrin $\alpha V\beta 3$ in complex with an Arg-Gly-Asp ligand," *Science*, vol. 296, no. 5565, pp. 151–155, 2002.

[23] H. A. Resing, "Apparent phase-transition effect in the NMR spin-spin relaxation time caused by a distribution of correlation times," *The Journal of Chemical Physics*, vol. 43, no. 2, pp. 669–678, 1965.

[24] Y. Gossuin, P. Gillis, A. Hocq, Q. L. Vuong, and A. Roch, "Magnetic resonance relaxation properties of superparamagnetic particles," *Wiley Interdisciplinary Reviews: Nanomedicine and Nanobiotechnology*, vol. 1, no. 3, pp. 299–310, 2009.


The Scientific
World Journal
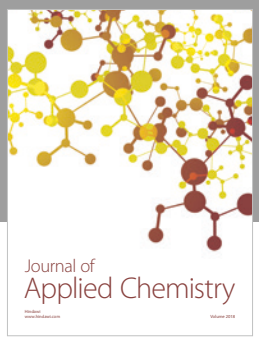
Journal of
Applied Chemistry
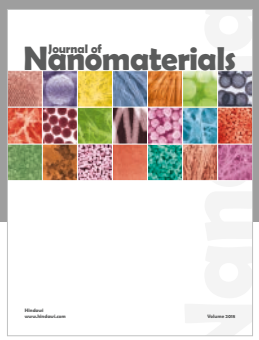
Journal of
Nanomaterials

Scientifica

International Journal of
Polymer Science
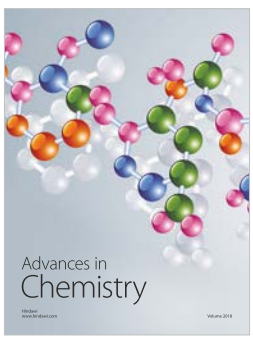
Advances in
Chemistry

Hindawi
Submit your manuscripts at
www.hindawi.com
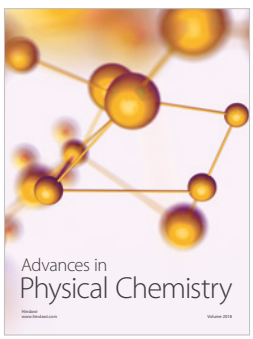
Advances in
Physical Chemistry

International Journal of
Analytical Chemistry
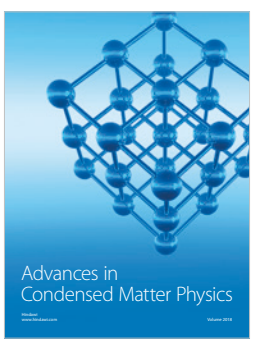
Advances in
Condensed Matter Physics
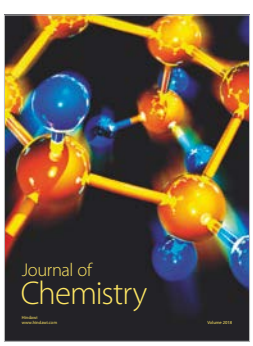
Journal of
Chemistry

International Journal of
Biomaterials
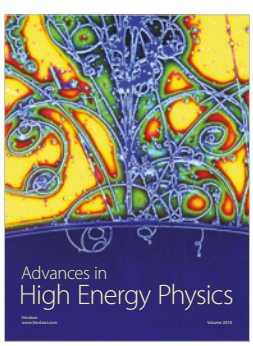
Advances in
High Energy Physics

Journal of
Engineering

Journal of
Nanotechnology

International Journal of
Corrosion

Journal of
Materials

BioMed
Research International
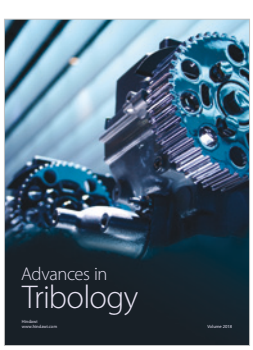
Advances in
Tribology
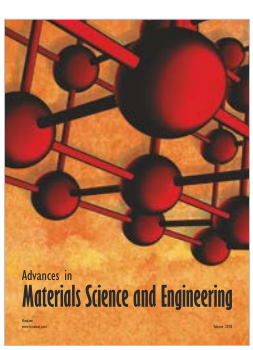
Advances in
Materials Science and Engineering